Journal of Hydrosciences and Environment
Available online at http://jhe.usb.ac.ir/

ISSN: 2345-5608

Monitoring the Land Subsidence and its Associated Landforms Using Remote Sensing Techniques in Feyzabad Plain (north-east Iran)

R. Zandi[1,*], K. Ghahraman[2], M. A. Zanganeh Asadi[3]

1,. Assistant Professor of Remote Sensing & GIS, Hakim Sabzevari University, Sabzevar, Iran.*

2. PhD student of Geomorphology, Eötvös Loránd University, Budapest, Hungary.

3. Associate Professor of Geomorphology, Hakim Sabzevari University, Sabzevar, Iran.

ARTICLEINFO

Article history:

Received: *21 August 2019*
Accepted: *22 December 2019*

Keywords:
Land subsidence,
Sentinel-1A,
Interferometry,
Feyzabad plain (Iran),
NDVI

ABSTRACT

This study characterizes land subsidence in Feyzabad plain, central Iran, using Sentinel-1A SAR data. These techniques are based on the analysis of pairs of synthetic aperture radar (SAR) images that are able to identify sub-centimeter changes in the line of sight (LOS) position of targets. Excessive groundwater withdrawal has caused several land subsidence in the studied area in the past few years. Using remote sensing techniques and SAR data, we analyzed the rate of land subsidence and its associated landforms in the area in a short time span. Feyzabad plain is located in an arid region with 154 mm annual precipitation. The most famous fault in the region is the Darouneh left-lateral fault with an east-west trend. To investigate land subsidence and the related effects, we first monitored ground motions between 2017 and 2018 in a 45-day period (for each pair of images) using SAR data and SNAP software. Then, we extracted linear landforms for each year to analyze subsidence in more details. We also mapped NDVI for both years so that we could compare the displacement and the vegetation cover in the studied area. Results showed that the maximum rate of subsidence was 3.9 cm in 2017 while the maximum rate in 2018 was 1.3 cm. NDVI maps revealed that decreasing pistachio cultivation has direct effects on the rate and magnitude of land subsidence. Results also showed that intensive subsides were centered in 2018 while in 2017, subsidence was scattered across the region.

1. Introduction

Land subsidence as a growing global problem is caused by several factors and many cities worldwide are suffering from this environmental and geological phenomenon (Du et al., 2018). The gentle down warping and sudden sinking of some segments of the ground surface are called land subsidence (Galloway and Burbey, 2011). Withdrawal of fluids such as groundwater, hydrocarbons and geothermal (Donaldson et al., 1995), aquifer-system compaction (Sneed and Galloway, 2000), underground mining (Dong et al., 2015), dewatering (oxidation) of peat or organic soils (Grzywna, 2017), crustal deformation (Antonellini et al., 2018), and hydrocompaction and sinkholes (Yechieli et al., 2016) are mentioned as the causes of land subsidence. Damaging to infrastructure and buildings, changes in elevation of water streams and other failures in aquifer system (Ruiz-Armenteros et al., 2018) are some of the results of land subsidence. Many researchers have been studied land subsidence in different aspects (Calderhead et al., 2011; Galloway and Burbey, 2011; Antonellini et al., 2018; Setyawan et al., 2015; Amighpey and Arabi, 2016; Wesatway, 2012). Although displacements are principally vertical, horizontal deformations can cause significant damages (Mahmoud pour et al., 2013). In recent years, many researchers have used remote sensing to determine the land subsidence in di fferent parts of the world (Van der Horst et al., 2018; Hay-Man NG et al., 2017; Yastika et al., 2018). Using this technology, we are able to monitor, predict and mitigate the disasters that land subsidence may cause (Yastika et al., 2018). It has been proved that Spaceborne SAR is a reliable technique to study ground motions in large areas (Ruiz-Armenteros et al., 2018). These techniques are based on the analysis of pairs of synthetic aperture radar (SAR) images that are able to identify sub-centimeter changes in the line of sight (LOS) position of targets (Sowter et al., 2016). Almost all of the plains of Iran suffer from subsidence. Based on numerous studies carried out in different plains in Iran, the over-extraction of groundwater can be named as the main factor of subsidence in plains of Iran. Fayzabad plain is one of the fertile areas in Khorasane-Razavi province, like other plains of Iran, experiences severe land subsidence. In this paper, first we estimate and analyze ground motion between the years 2017 to 2018, using sentinel 1-A SAR interferometry, to monitor the subsidence in a year. Since land subsidence is a dynamic phenomenon and, in addition, many researchers have been studied it over long periods of time, we decided to review the subsidence in the Feyzabad area

* Corresponding author's email:
r.zandi@hsu.ac.ir

in the short term. However, the long-term effects of this land subsidence may be significant, Short-term changes are particularly important as an environmental hazard. We also extract linear landforms made by land subsidence in the area using Landsat images. The consequences of land subsidence in the study area in tow main forms, longitudinal cracks and deep holes. They have different geometry and development status.

2. Materials and methods

2.1. Study area

The study area is located in central Iran, between longitudes 57° 58' E to 59° 03' E and latitudes 34° 48' N to 35° 11' N in Razavi Khorasan province (Fig.1). The climate of the study area is arid and semiarid. The mean annual temperature is 17.4° C and the average annual rainfall is 154 mm (Parsasadr et al., 2016). The oldest geological outcrops in the study area belong to Cambrian (Kalshaneh formation) and the youngest formations are quaternary sediments, located in the center of the plain. There are three main faults in the region, which are 1) Taknar fault 2) Daruneh fault and 3) Kuh Faghan fault. The geological characteristics of the Feyzabad region indicate that fault movements have played an important role in the formation of sedimentary basins changes. Maybe the most important active fault in the region is Daruneh left-lateral fault with an east to west trend. It passes through the center of the Feyzabad region. The area is 470 square kilometers.

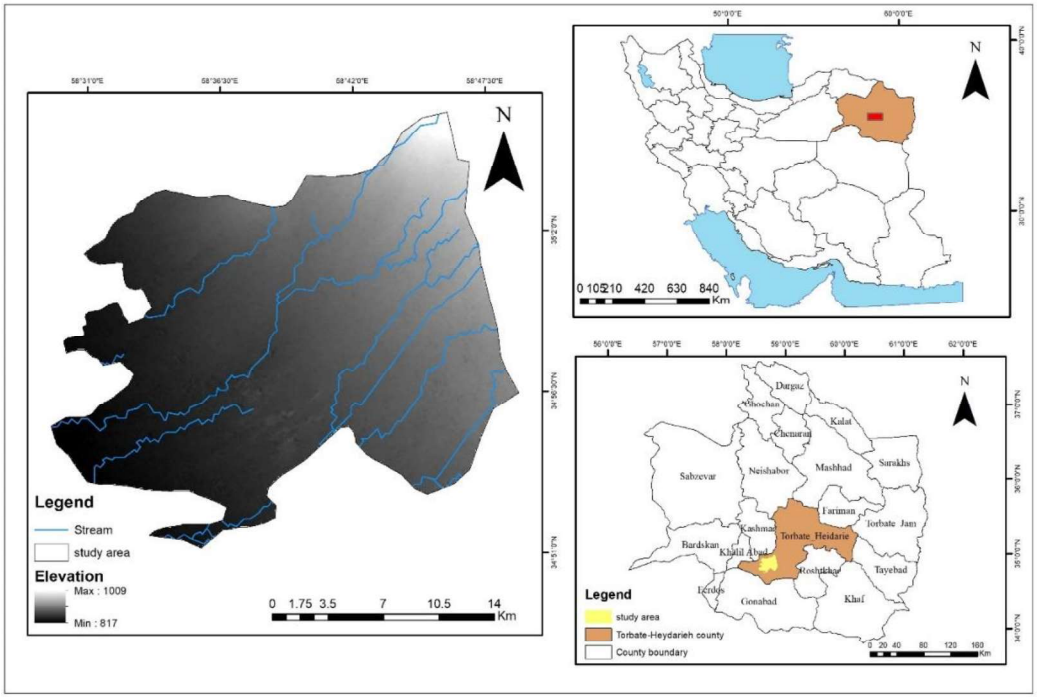


Fig. 1. The geographical location of the studied area in eastern Iran

Fig. 2 shows the geological setting of the study area and part of the upland mountainous area. The plain itself is covered by quaternary deposits including recent alluvium (Qal), clay flat (Qc), young gravel fans (Qt2) and older terraces and gravel fans (Qt1). Other lithological units in the upland mountainous area are reddish sandstone and conglomerate (Ng_{cs}), brown conglomerate (Ng_c), limestone (Db) and brown-reddish sandstone and dolomite (Sp). Generally, the Feyzabad aquifer is an unconfined aquifer surrounding by mountains, with a range of 60 to 200-meter alluvium thickness (Parsasadr et al., 2016).

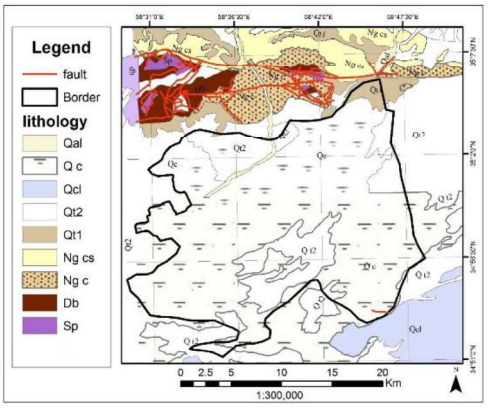


Fig. 2. Geological setting of the study area

2.2. Methods

The methodology is shown in Fig. 3 and described in detail in the following.

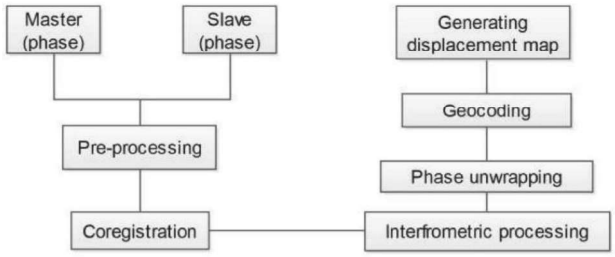


Fig.3. Flow chart the methodology to create a displacement map

2.2.1. Satellite images

Sentinel-1A, which is a space mission of the Europe Space Agency of the Copernicus Program, was launched on April 3, 2014 (Dai et al., 2016). The new type of scanSAR mode in sentinel 1A, known as TOPS SAR, has the resolution of about 3.5 m in the range direction and 14 m in azimuth direction to scan SAR, but it also has an enhanced single-to-noise ratio distribution et al., 2015). We used two pairs of images taken over a period of about 45 days for each pair in this study. Details of the images are shown in Table 1. The level-1 images were downloaded from the Sentinel-1 Scientific Data Hub. VV polarization mode is used in all images. We also used the Snap software to achieve the amount of land subsidence and for the interferometry processes.

2.3. Interferometric processing chain

2.3.1. Pre-processing

Since the study area is included in 3 bursts of the sentinel-1 image, there is no need to process all the bursts. Because the extraction of Sentinel-1 TOPS bursts will be made per acquisition and per sub-swath and this will take a long time and to focus only over the study area, first we split each image into 3 bursts (Fig. 4).

2.3.2. Co-registration

In the first processing step, we applied orbit files in S-1 products to provide accurate satellite position and velocity information. Then we co-registered the two sentinel images for each year. In this step, the second image (slave) will be co-registered with respect to the first image (master) (Fig. 5). Back geocoding tool in snap software co-registers tow S-1 products using the orbits of the two products and a Digital Elevation Model (DEM).

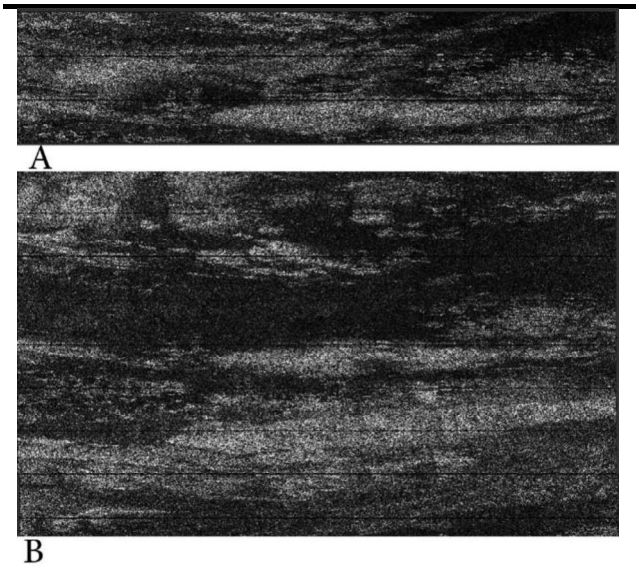


Fig. 4. Difference between split applied image (A) and original image (B)

In the last step in co-registration, we used ESD (Enhanced-Spectral-Diversity) to exploit the data at the overlapped area of the adjacent burst and then it performs range and azimuth correction of every burst.

2.3.3. Interferometric Processing

As the first step at this stage, we produced an interferogram between the master and slave images that we already co-registered. The next step was to deburst interferograms. The next step was to remove the topographic induced phase from the debursted interferogram. As the original SAR image contains inherent speckle noise, we used multilook process to reduce the speckle appearance and to improve the image interpretability. Then we performed phase filtering of the interferogram in order to reduce phase noise (Fig. 6). The filtering method we implemented was Goldstein method proposed by Goldstein & Werner in 1998. The final step in Interferometric processing part was to export the data for SNAPHU processing in order to apply phase unwrapping.

2.3.4. Phase Unwrapping

After unwrapping in the Linux, the next step was to import the results from SNAPHU processing and to construct the Interferometric product that contains the unwrapped phase band and the metadata of the source interferometric product. Then we converted the interferometric phase to the displacement map.

2.3.5. Geocoding

Since SAR images have topographical variations of a scene and the tilt of the satellite sensor, distances can be distorted. Terrain corrections were intended to compensate for these distortions so that the geometric representation of the image will be as close as possible to the real world. To

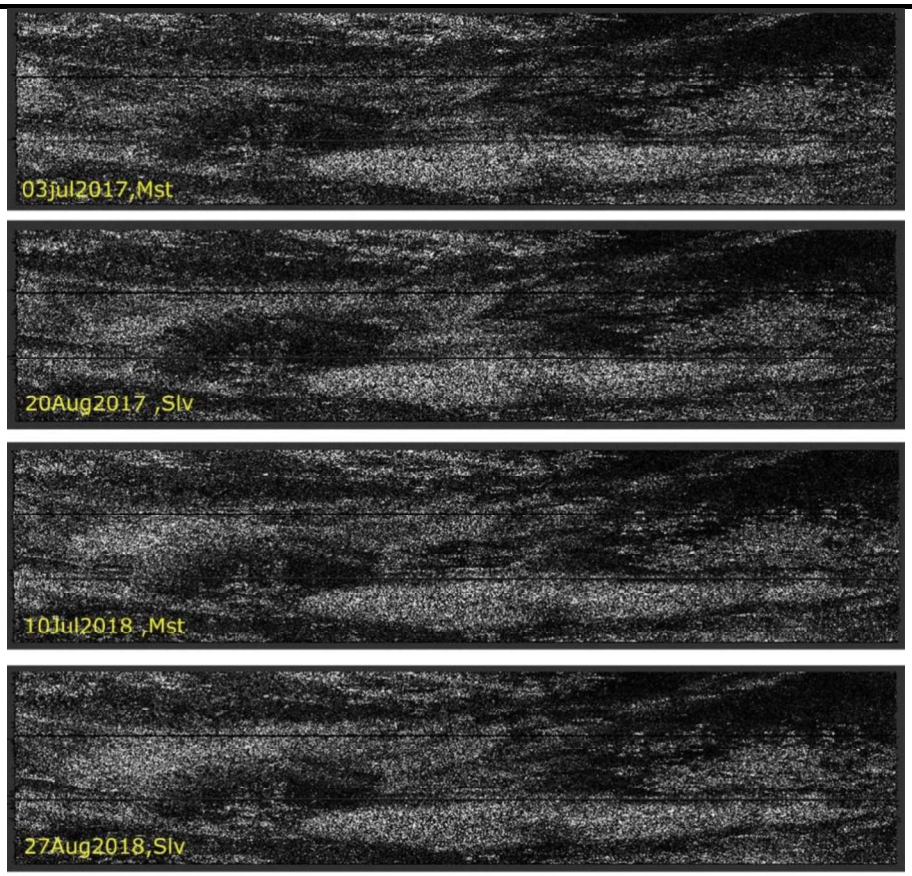


Fig. 5. Master and slaves images separately

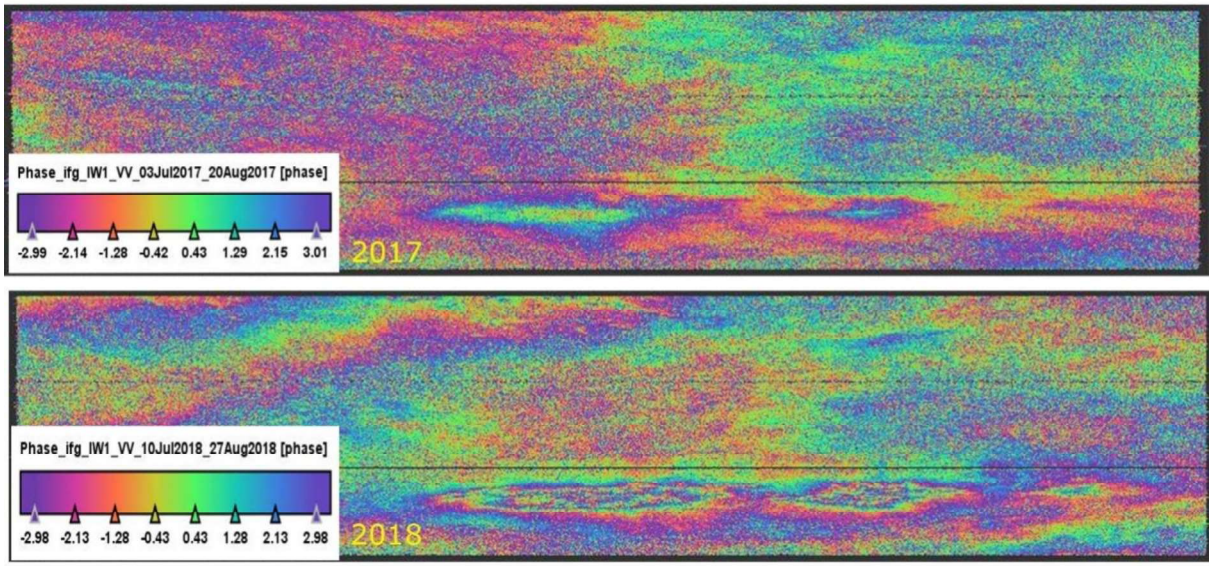


Fig. 6. Interferograms of the studied area

geocode the Sentinel-1 products we used the Range Doppler Terrain Correction.

2.4. Extraction of linear landforms

When land subsidence occurs in an area, longitudinal cracks are expected. To find out if there is any relationship between land subsidence and longitudinal cracks in the

study area, we extracted the linear features using Landsat 8 satellite imagery. Landsat 8 satellite has 11 bands, with band 1 to 7 having a resolution of 30 meters, while band 8 has a resolution of 15 meters. We first used ENVI software to increase the resolution of bands 1 to 7 to 15 meters based on band 8 resolution. Then using PCI GEOMATICA we extracted the linear features in the study area. We also used Landsat 8 images to extract NDVI[1] for the studied area to compare the vegetation changes in the studied period. To create an NDVI map (Fig. 10) we used near-infrared and red bands (band 4 and band 5) in Landsat 8 images corresponding to the year in question.

3. Results and Discussion

3.1. First period (2017/7/3 to 2017/8/20)

Bing located in a region with low rainfall (Fig. 8), far from the sea and near the desert and also with the lack of surface flows, groundwater is the primary water source in the studied area and this leads to over-extraction of groundwater which in turn is the main reason of subsidence in the region. As mentioned earlier, many studies in different plains in Iran showed that the main reason for subsidence in the country is the excessive groundwater extraction. There is no doubt that over-extraction of groundwater has led to land subsidence in Feyzabad plain as well. The profitable trade of pistachios in the area is also an important agent for over-extraction. As shown in Fig. 7 (Top), in 2017, the entire region suffered land subsidence at different rates. The maximum rate is -3.9 centimeters and the lowest is -1 centimeter. The negative sign in the legend indicates that the subsidence has happened. If we divide the area from top to bottom into three parts, the most intense subsides have occurred in the middle section (Fig. 7.Top). As far as the center goes out, the amount of land subsidence decreases which means it is happening at a lower rate. In terms of area, 15 percent (table 1) of land subsidence has happened at the rate of -2.5 Cm which includes the widest area. At the North West, the least amount of subsidence is detectible. Generally, in 2017, classes between the rates of -2.7 to -2.2 have the widest area of land subsidence, although just 3.96 percent of the area face intense subsidence. In 2017 the total length of linear features created by subsidence in the study area was 658.420 km (Table 1). We can find these cracks almost everywhere, especially in the areas with the highest rate of subsidence (Fig. 8). The study of average annual precipitation data in two meteorological stations close to the studied area (Torbat-e-Heydarieh and Kashmar Stations) represents an average of 12mm annual precipitation in Kashmar and 15mm in Torbat-e-Heydarieh in 2017 as well (Fig. 9). Unfortunately, precipitation data for 2018 was not available. Geologically speaking, in both studied periods land subsidence has occurred in Qt[2] and Qc which represent find grading quaternary sediments and includes cultivated areas.

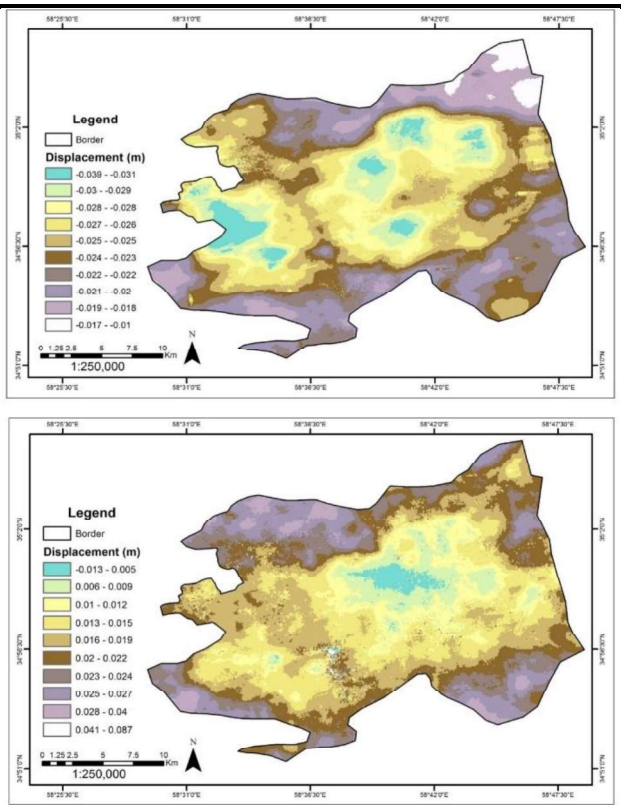


Fig. 7. Displacement map of the study area. Top: the displacement map in 2017. Bottom: the displacement map in 2018.

Negative numbers donate the rate of subsidence. Blue spots show the most intensive displacements. In 2017 there are different spots extended in the area but in 2018 there is just one huge spot in the center of the studied area.

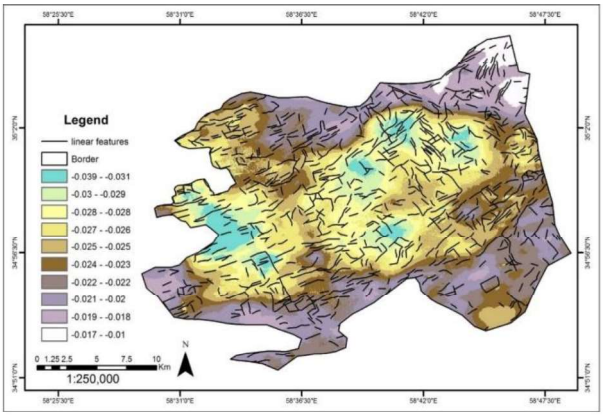
Table 1. Displacement area and linear feature length in 2017

Displacement Rate (cm)	Area (Km^2)	Area (percent)
(-3.9) – (-3.1)	18.64	3.96
(-3) – (-2.9)	34.90	7.42
(-2.8) – (-2.8)	49.24	10.46
(-2.7) – (-2.6)	65.30	13.87
(-2.5) – (-2.5)	73.50	15.61
(-2.4) – (-2.3)	60.86	12.93
(-2.2) – (-2.2)	65.46	13.91
(-2.1) – (-2)	59.03	12.54
(-1.9) – (-1.8)	33.02	7.01
(-1.7) – (-1)	10.77	2.29
Total line features length (km)	**658.420**	**100**

[1] Normalized Difference Vegetation Index

3.2. Second period (2018/7/10 to 2018/8/27)

While in 2018 there is still land subsidence in the area, its size and area have been reduced. The most intense subsidence in 2018 was -1.3 cm which occurred in 2 percent of the area. As shown in Fig. 7 (Bottom), intense subsidence areas in 2017 are disappeared in 2018. The subsidence has occurred in the central area and other areas had positive displacement. Displacement rates of -1.6 to -2.2 represent more than 30% of the area (Table 2). Linear features length decreased to 605.882km in total. The displacement map (Fig. 5) reveals that the spatial pattern of subsidence as changed so that high-rate subsidence points are scattered throughout the region in 2017 while high rate points are concentrated in one area the following year. As evidenced by the data, the highest rates of subsidence occurred in agricultural areas that water extraction is common there and cause that land to rupture. Generally, all of the plains in Iran have been facing subsidence with different rates in recent years. Amighpay and Arabi (2016) reported a 12 cm/yr (peak amplitude) rate of subsidence in Yazd-Ardakan plain. A study carried out by Mousavi et al. (2001) in Rafsanjan plain estimated the rate of subsidence as much as 10 cm in a 70 day period. The reported that over-extraction of groundwater for irrigation (mainly pistachio) has led to a sharp decrease in regional groundwater (15 meters between 1971 and 2001). Mahmoud pour et al. (2013) reported 36 cm/yr subsidence for Tehran plain. There are many other studies illustrating the critical condition of the Iranian plains regarding the land subsidence. Average annual subsidence in the Feyzabad Plain at a rate of about ~ 31.2 cm indicates the critical conditions and severe subsidence in this region.



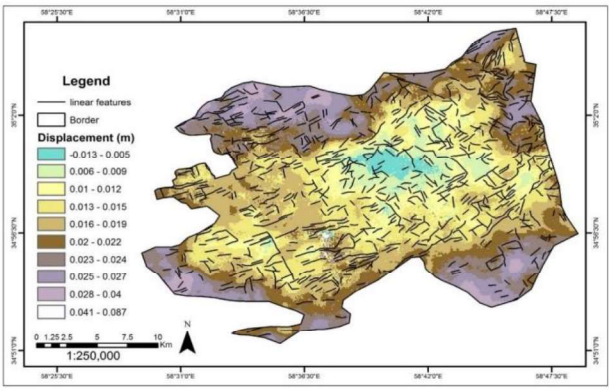


Fig. 8. Linear features map with the displacement map in background. Comparing both maps shows that in 2017 (top) due to land subsidence, linear features are visible in the whole area while in 2018 (bottom) areas with less subsidence show fewer lines.

Although anthropogenic agents may have been involved in reducing linear features length, yet it is a good testifier for less displacement in 2018. A decrease in cultivation, reduced groundwater extraction, more precipitation in 2018, increasing local awareness about land subsidence are possible reasons for the decrease in displacements. The NDVI map of the study area (Fig. 10) also shows a decrease in the area under cultivation in 2018 compared to 2017.

Table 2. Displacement area and linear feature length in 2018

Displacement Rate (cm)	Area (Km^2)	Area (percent)
(-1.3) – (0.5)	10.50347	2.16
(0.6) – (0.9)	31.17267	6.41
(1) – (1.2)	44.85082	9.22
(1.3) – (1.5)	67.91792	13.97
(1.6) – (1.9)	74.60502	15.34
(2) – (2.2)	76.73273	15.78
(2.3) – (2.4)	61.95695	12.74
(2.5) – (2.7)	58.78227	12.09
(2.8) – (4)	47.39226	9.75
(4.1) – (8.7)	12.37788	2.55
Total line features length	605.882	100

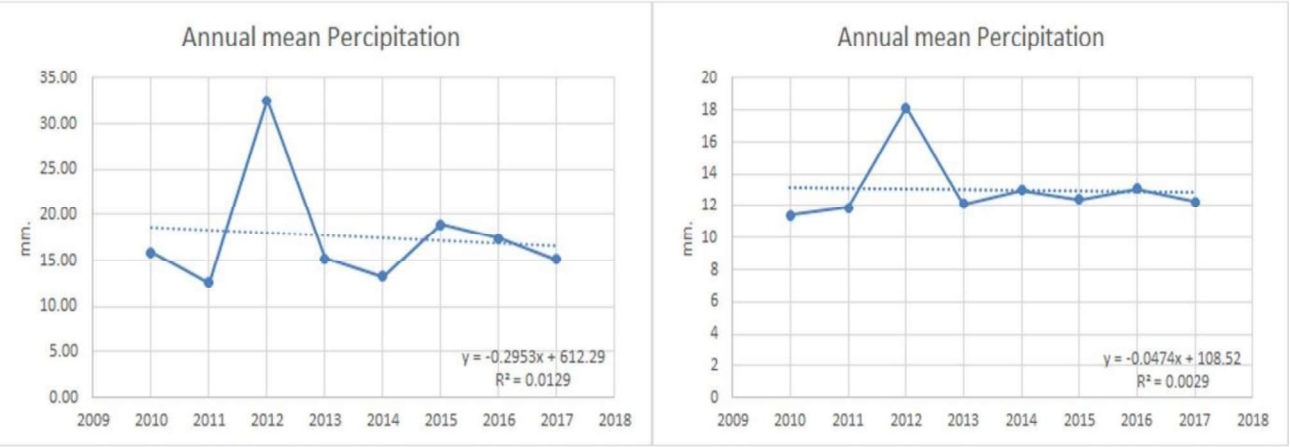


Fig. 9. Mean annual precipitation in nearest stations (Torbat-e-Heydarieh on the left and Kashmar on the right)

Low values of NDVI (> 0.1) corresponds to bare lands without vegetation cover, while moderate values (0.2 - 0.3) represent shrubs and grasslands. High values (0.6 - 0.8) indicate dense vegetation covers (temperate and tropical rainforests) (Xie et al., 2010). The area and the area percentage of the NDVI classification are given in table 3. Approximately 45 percent (~212 Km^2) of the study area is in the moderate vegetation class (0.1 – 0.3) in 2017 (Table 3). Although areas in this class are scattered throughout the region, the central and upper parts of the region show more density (Fig. 10A). Fig. 10 Shows that in 2018, ~85 percent of the area fits in the low value class (0.06 – 0.19) whereas just 3.56 percent of the area has moderate vegetation cover which means less cultivation in that year. As Fig. 7 shows, areas with the highest rate of subsidence in 2018 are located in the central part of the region and according to the NDVI map (Fig. 10), the moderate vegetation cover is in the same area as well. Overall, the results of this study showed the rate of subsidence in a short term period and the effect of less cultivation on reducing the subsidence rate.

Table 3. Area and area percentage of the NDVI classes in 2017 and 2018

Normalized Difference Vegetation Index for 2017		
Class	Area (Km^2)	Area %
> - 0.1	256.734	54.543
0.1 – 0.3	212.697	45.188
0.3 – 0.5	1.257	0.267
1	0.010	0.002
Normalized Difference Vegetation Index for 2018		
-0.07 – 0.06	51.596	10.96
0.06 – 0.19	402.288	85.47
0.19 – 0.33	16.744	3.56
0.33 – 0.47	0.072	0.02

As a result of land subsidence in the region numerous deep pits, with different sizes, have been created as well as longitudinal cracks (Fig. 11). These pits and longitudinal cracks pose a great threat to residents, infrastructure, roads and more. We also showed the linear features of subsidence and their density and the differences in the studied area. NDVI maps showed that decreasing in pistachio cultivation has direct effects on the rate and magnitude of land subsidence (Fig. 10).

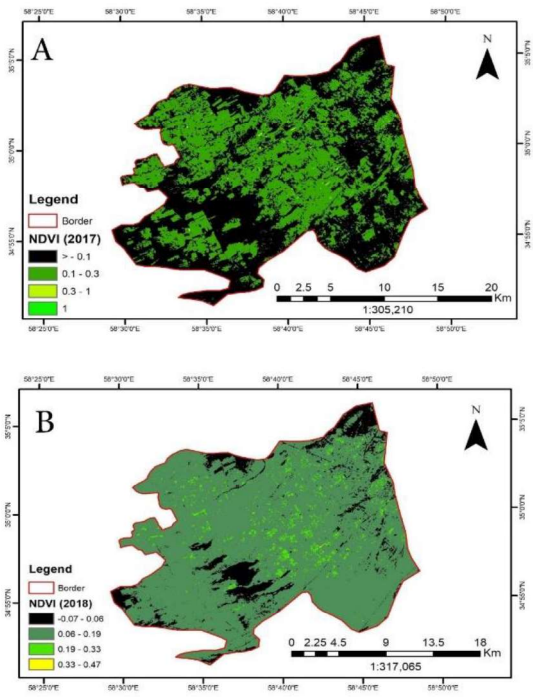


Fig. 10. Normalized Difference Vegetation Index of the study area. A) NDVI in 2017 that shows the vegetation density in the central and upper part of the region. B) NDVI in 2018 that represents the sharp decrease in moderate vegetation cover. Most of the remaining cultivation in 2018 is in the central part of the region.



Fig. 11. subsidence feature examples in Fayzabad plain. A) A new hole which is not developed yet. B) One of the longest linear features in the area. C: a developing linear feature.

4. Conclusion

Over the past few years, land subsidence has led to significant damages in Fayzabad plain. In this study, we used sentinel 1-A SAR images to investigate and compare the rate of subsidence in Fayzabad plain. We also extracted linear features using Landsat images. To show the difference in vegetation cover we create NDVI maps using Landsat 8 images. Based on displacement maps, the maximum rate of subsidence was 3.9 cm in 2017 while the maximum rate in 2018 was 1.3cm in almost 45 days period.

The results revealed that the most intense rates were in cultivated areas which are located in the central and upper parts of the studied area. In terms of spatial distribution, in 2017, subsidence was scattered across the region however in 2018, the most important subsidence zone is located in the center of the region. A comparison of NDVI maps and displacement maps shows that subsidence zones correspond to areas with high-density vegetation cover. In 2018, as the vegetation declines, the rate of subsidence declines in terms of rate and only the central part, which has vegetation cover, indicates subsidence. Since the main cause of subsidence in most plains of Iran has been reported due to groundwater over-extraction, it is recommended to use methods such as changing the cropping pattern, aquifer restoration plans, informing residents and…to change the situation so as to compensate for a fraction of the lost groundwater.

5. References

1. Amighpey, M., & Arabi, S. (2016). Studying land subsidencein Yazdprovince, Iran, by integration. Remote Sensing Applications: Society and Environment, 4, 1-8.

2. Antonellini, M., Giambastiania, B., Greggiob, N., b, Bonzic, L., Calabresec, L., Severic, P. (2018). Processes governing natural land subsidence in the shallow coastal aquifer. Catena, 172, 76-86.

3. Calderhead, A. I., Therrien, R., Rivera, A., & Garfias, J. (2011). Simulating pumping-induced regional land subsidence with the use of InSAR and field data in the Toluca Valley, Mexico. Adv. Water resource, 34, 83-79.

4. Dai, K., Li, z., Tomás, R., Liu, G., Yu, B., Wang, X., Stockamp, J. (2016). Monitoring activity at the Daguangbao mega-landslide (China) using Sentinel-1 TOPS time series interferometry. Remote Sensing of Environment, 186, 501-513.

5. Donaldson, E., Chilingarian, G., & Yen, T. (1995). Subsidence due to fluid withdrawal. Elsevier science, 41, 497.

6. Dong, S., Samsonov, S., Yin, H., Yao, S., & Xu, c. (2015). Spatial-temporal analysis of ground subsidence due to underground coal mining in Huainan coalfield, China. Environ. Earth Sci, 73, 5523-5534.

7. Du, Z., Ge, L., Hay-Man Ng, A., Zhu, Q., Yang, X., & Li, L. (2018). Correlating the subsidence pattern and land use in Bandung, Indonesia with both sentinel-1/2 and ALOS-2 satellite images. Int J Appl Earth Obs Geoinformation, 67, 54-68.

8. Farkas, P., Hevér, R., & Grenerczy, G. (2015). Geodetic integration of Sentinel-1A IW data. EGU General Assembly Conference Abstracts, (p. 13483).

9. Galloway, D., & Burbey, T. (2011). Regional land subsidence accompanying groundwater extraction. Hydrogeol, 19, 1459-1486.

10. Goldstein, R.M., Werner, C.L., (1998). Radar interferogram filtering for geophysical applications. Geophys. Res. Lett. 25, 4035–4038.

11. Grzywna, A. (2017). The degree of peatland subsidence resulting from drainage of lan. Environ. Earth Sci., 76, 559.

12. Hay-Man Ng, A., Ge, L., Du, Z., Wang, S., & Ma, C. (2017). Satellite radar interferometry for monitoring subsidence induced by long wall mining activity using Radarsat-2, Sentinel-1 and ALOS-2 data. Int J Appl Earth Obs Geoinformation, 61, 92-103.

13. Mahmoud pour, M., Khamehchiyan, M., Nikudel, M., & Ghassemi, M. (2013). Numerical simulation and

prediction of regional land subsidence caused by groundwater exploitation in the southwest plain of Tehran, Iran. Engineering Geology, 201, 6-28.

14. Mousavi, S.M., Shamsai, A., Naggar, M.H.Z., Khamehchiyan, M., (2001). A GPS-based monitoring program of land subsidence due to groundwater withdrawal in Iran, Canadian Journal Civil Engineering, 28(3): 452-462.

15. Parsasadr, H., Nikpeyman, V., & Nassery, H. (2016). Management of groundwater resources of Mahvelat-Faizabad aquifer and evaluation of extent of saline water zone using numerical simulation. Water Harvesting Research, 1, 52-62.

16. Ruiz-Armenteros, A., Lazecky, M., Ruiz-Constán, A., Bakoň, M., Delgado, M., Sousa, J., Perissin, D. (2018). Monitoring continuous subsidence in the Costa del Sol (Málaga province, southern Spanish coast) using ERS-1/2, Envisat, and Sentinel-1A/B SAR interferometry. Procedia Computer Science, 138, 354–361.

17. Setyawan, a., Fukuda, Y., Nishijima, J., & Kazama, T. (2015). Detecting Land Subsidence Using Gravity Method in Jakarta and. Procedia Environmental Sciences, 23, 17-26.

18. Sneed, N., & Galloway, D. (2000). Aquifer-system compaction and land subsidence: measurements, analyses, and simulation- the holly site, Edward Air force base, Antelope Valley, California. U.S geological survey water resources Investigation report, 70.

19. Sowter, A., Amat, M., Cigna, F., Marsh, S., Athab, A., & Alshammari, L. (2016). Mexico City land subsidence in 2014–2015 with Sentinel-1 IW TOPS: Results using the Intermittent SBAS (ISBAS) technique. International Journal of Applied Earth Observation and Geoinformation, 52, 230–242.

20. Van der Horst, T., Rutten, M., van de Giesen, N., & Hanssen, R. (2018). Monitoring land subsidence in Yangon, Myanmar using Sentinel-1 persistent. Remote Sensing of Environment, 217, 101-110.

21. Westaway, R. (2012). A numerical modelling technique that can account for alternations of uplift and. Geomorphology, 165-166, 124-143.

22. Xie, Y., Zhao, X., Li, L., Wang, H., (2010). Calculating NDVI for landsat7 ETM data after atmospheric Correction using 6s model: a case study in Zhangye city, china, IEEE Geo Informatics 18th international conference, pp. 1-4.

23. astika, P., Shimizu, N., & Abidin, H. (2018). Monitoring of long-term land subsidence from 2003 to 2017 in coastal area of Semarang, Indonesia by SBAS DInSAR analyses using Envisat-ASAR, ALOSPALSAR, and Sentinel-1A SAR data. Advances in Space Research.

24. Yechieli, Y., Abelson, M., & Bear, G. (2016). Sinkhole formation and subsidence along the Dead Sea coast, Isreal. Hydrogeol. J., 24, 601-612.